

## Structure Elucidation

International Edition: DOI: 10.1002/anie.201611051

German Edition: DOI: 10.1002/ange.201611051

# A Reactive, Rigid Gd<sup>III</sup> Labeling Tag for In-Cell EPR Distance Measurements in Proteins

Yin Yang<sup>+</sup>, Feng Yang<sup>+</sup>, Yan-Jun Gong, Jia-Liang Chen, Daniella Goldfarb,<sup>\*</sup> and Xun-Cheng Su<sup>\*</sup>

**Abstract:** The cellular environment of proteins differs considerably from *in vitro* conditions under which most studies of protein structures are carried out. Therefore, there is a growing interest in determining dynamics and structures of proteins in the cell. A key factor for *in-cell* distance measurements by the double electron–electron resonance (DEER) method in proteins is the nature of the used spin label. Here we present a newly designed Gd<sup>III</sup> spin label, a thiol-specific DOTA-derivative (DO3MA-3BrPy), which features chemical stability and kinetic inertness, high efficiency in protein labelling, a short rigid tether, as well as favorable spectroscopic properties, all are particularly suitable for *in-cell* distance measurements by the DEER method carried out at W-band frequencies. The high performance of DO3MA-3BrPy-Gd<sup>III</sup> is demonstrated on doubly labelled ubiquitin D39C/E64C, both *in vitro* and in HeLa cells. High-quality DEER data could be obtained in HeLa cells up to 12 h after protein delivery at *in-cell* protein concentrations as low as 5–10 μM.

Characterization of the dynamics, interactions and structures of proteins is an important way of delineating their functions. Current biophysical methods used to explore protein dynamics and structures are generally applied *in vitro*, under conditions that differ considerably from the cellular milieu. In the cell, molecular crowding, sub-organelle localization, post-translational modifications, and specific and non-specific associations with cellular components may inevitably affect the structure and conformational equilibria of proteins.<sup>[1]</sup> Therefore, effective methods for exploring the atomic resolution structure and dynamics of proteins in their native cellular environment are highly desirable. Currently, NMR spectroscopy is probably the most effective method for determining structure and dynamics in the cell at atomic resolution. However, its low sensitivity invariably requires expensive isotope labeling and high protein concentrations,

and it is generally applicable to a limited number of proteins.<sup>[1a,2]</sup> DEER is a method that provides distance distributions between pairs of, usually identical, spin labels that are attached to a bio-macromolecule at well-defined sites.<sup>[3]</sup> Its distance accessibility is usually in the 1.6–8 nm range<sup>[3]</sup> and can increase to 16 nm if the protein is deuterated.<sup>[4]</sup> Owing to its inherently high absolute sensitivity as compared with NMR spectroscopy, and its insensitivity to protein size and background signals, DEER can become an efficient method for *in-cell* structural studies of proteins.<sup>[5]</sup>

The first *in-cell* DEER experiments using standard nitroxide spin labels were reported in oocytes, where the low stability of the nitroxide radicals in the reducing cellular environment was noted.<sup>[5a]</sup> This is not a problem when the nitroxide spin label is exposed to the outside of the cell environment,<sup>[6]</sup> but otherwise it pauses a significant limitation on this methodology. Thus, for the *in-cell* DEER method to become a significant and viable technique, stable spin labels are required to explore the protein interactions and dynamics in the cell. New nitroxide spin labels are currently under development but so far they have not been demonstrated in *in-cell* DEER experiments.<sup>[7]</sup> Recently, RIDME distance measurements between a trityl spin label and intrinsic Fe<sup>III</sup> in CP450, requiring 80 h accumulation time, was reported in oocytes.<sup>[8]</sup> An attractive alternative approach is to use Gd<sup>III</sup>-based spin labels, which have already been reported for many *in vitro* Gd<sup>III</sup>–Gd<sup>III</sup> DEER applications.<sup>[9]</sup>

We have recently reported on *in-cell* W-band Gd<sup>III</sup>–Gd<sup>III</sup> DEER distance measurements of maleimide-DOTA-Gd<sup>III</sup>-labeled proteins in human HeLa cells.<sup>[10]</sup> The drawback of the maleimide-DOTA tag is its rather long and flexible tether. In addition, there were reports that thiomaleimide conjugates do not exhibit long-term stability in cells due to the thiol exchange with glutathione and the hydrolysis of succinimide ring.<sup>[11]</sup> Q-band DEER experiments on a 4-vinyl PyMTA-Gd<sup>III</sup> conjugated peptide injected into oocytes was reported as well.<sup>[12]</sup> However, the low reactivity of this tag towards protein thiols results in unfavorable labeling conditions for a protein.<sup>[13]</sup> More recently, a lanthanide binding peptide was fused into a helical bundle peptide both at the N- and C-termini, Gd<sup>III</sup> was supplemented with high concentration (100 to 500 μM) through the growing media and W-band *in-cell* spectra were recorded.<sup>[14]</sup> The main problem with this approach is the low binding constant of Gd<sup>III</sup> and the long measurement time (72 h) owing to the background of large amounts of free Gd<sup>III</sup>, which affects the signal-to-noise ratio.

In general, efficient *in-cell* DEER measurements require high stability of the spin label, a stable linker between the protein of interest and the spin label and a minimal size of the

[\*] Dr. Y. Yang,<sup>[†]</sup> Prof. D. Goldfarb  
Department of Chemical Physics  
Weizmann Institute of Science  
Rehovot 76100 (Israel)  
E-mail: daniella.goldfarb@weizmann.ac.il

F. Yang,<sup>[†]</sup> Y. J. Gong, J. L. Chen, Prof. X.-C. Su  
State Key Laboratory of Elemento-organic Chemistry  
Collaborative Innovation Center of Chemical Science and  
Engineering (Tianjin), Nankai University  
Tianjin 300071 (China)  
E-mail: xunchengsu@nankai.edu.cn

[†] These authors contributed equally to this work.

Supporting information for this article can be found under:  
<http://dx.doi.org/10.1002/anie.201611051>.

spin label that will not affect the protein structure. Finally, the linker should be short and rigid for obtaining a narrow distance distribution that does not mask protein conformational changes.

The formation of a thioether bond between a protein and a Gd<sup>III</sup> spin label is a promising way to introduce a paramagnetic center in a protein for in-cell studies.<sup>[10,12]</sup> The stable C–S bond can be generated by either a nucleophilic substitution reaction between the solvent-exposed protein thiols and haloacetamide derivatives,<sup>[15]</sup> phenylsulfonyl<sup>[16]</sup> or nitro-substituted pyridines,<sup>[17]</sup> methylsulfonylbenzothiazole derivatives,<sup>[18]</sup> or a Michael addition-like thiol-ene reaction.<sup>[19]</sup> The single-armed (4-phenylsulfonyl) pyridine-substituted DOTA-like tags (DO3MA-Py, Py represents the 4-phenylsulfonyl pyridine) were demonstrated as stable and rigid paramagnetic tags in protein analysis by paramagnetic NMR spectroscopy both in vitro and in living cells.<sup>[20]</sup> The coordination of the pyridine nitrogen to the metal ion restricts the flexibility of the spin label and hence, it should report narrower distance distributions in DEER measurements compared with the maleimid-DOTA tag. However, the low reactivity of these DO3MA-Py tags requires a high pH (ca. 9)<sup>[20a]</sup> or a high temperature and a long incubation time (40 °C and 20 hours, respectively)<sup>[20b]</sup> for protein modifications. These conditions are not suitable for efficient and general protein modifications. Here we present a new reactive thiol-specific DOTA-derivative, (2*R*,2'*R*,2''*R*)-2,2',2''-(10-(5-bromo-4-(phenylsulfonyl)pyridin-2-yl)methyl)-1,4,7,10-tetraazacyclododecane-1,4,7-triyl)tripropanoic acid (DO3MA-3BrPy) (Figure 1), for efficient in-cell DEER measurements, as demonstrated on ubiquitin in human HeLa cells.

The synthesis of the DO3MA-3BrPy tag and the formation of the Gd<sup>III</sup> complex are given in the Supporting Information. A double cysteine mutant of ubiquitin, D39C/E64C, was expressed and purified. The ligation of DO3MA-3BrPy-Gd<sup>III</sup> with D39C/E64C ubiquitin at pH 8 was completed within six hours at room temperature with a ligation yield of about 80 % (see the Supporting Information). This is significantly faster than the previously reported 4PhSO<sub>2</sub>-PyMTA, DO3MA-Py, and DO8M-Py tags.<sup>[16,20]</sup> The increased reactivity of DO3MA-3BrPy-Gd<sup>III</sup> towards solvent exposed cysteines, imparted by the Br substitution is consistent with earlier findings.<sup>[21]</sup>

In vitro paramagnetic NMR measurements were carried out on the DO3MA-3BrPy-Yb<sup>III</sup>-tagged single and double cysteine mutants, D39C, E64C, and D39C/E64C to ensure

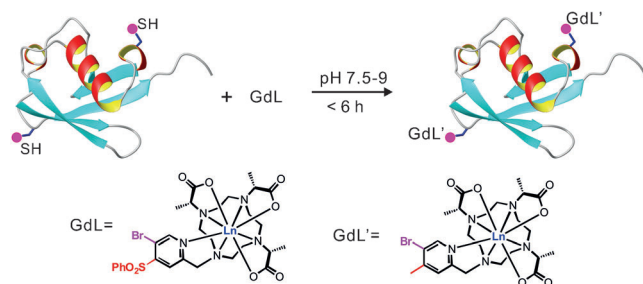


**Figure 1.** An efficient way of tagging proteins with a stable and rigid Gd<sup>III</sup> tag for in-cell DEER measurements.

that the labeling does not affect the protein structure and to assess the mobility of the spin label in the protein conjugate (Figures S3–6 and Table S1). High-resolution spectra were recorded and analyzed with <sup>15</sup>N-labeled protein samples. Large pseudo-contact shifts (PCSs) were generated for the D39C-DO3MA-3BrPy-Yb<sup>III</sup> and E64C-DO3MA-3BrPy-Yb<sup>III</sup> adducts, and similar paramagnetic tensors were determined for the two protein adducts (using the Numbat program<sup>[22]</sup>). The large PCS and the paramagnetic susceptibility tensor parameters (Table S1) suggest that the protein-DO3MA-3BrPy-Ln<sup>III</sup> conjugate is rigid. The excellent agreement between the experimental and back-calculated PCSs indicates reliable paramagnetic tensors in the two protein conjugates (Figure S6), and that no significant structural perturbations are observed when the paramagnetic tag is introduced. Similar measurements were carried out on the doubly DO3MA-3BrPy-Yb<sup>III</sup> labeled <sup>15</sup>N-ubiquitin D39C/E64C sample. Comparison of experimental PCSs determined in the doubly labeled protein with the sum of PCSs from singly labeled protein samples gave a very good agreement. Compared with the singly labeled proteins, the high-quality correlation of the experimental data and the calculated PCSs from the individual paramagnetic tensors indicate that there are no obvious structural variations in the doubly labeled D39C/E64C adduct (Figure S6).

Following the encouraging results from the in vitro NMR characterization, we proceeded to in vitro and in-cell DEER measurements. The doubly DO3MA-3BrPy-Gd<sup>III</sup>-labeled protein was delivered by hypotonic swelling<sup>[23]</sup> and electroporation<sup>[10a]</sup> into HeLa cells. Echo-detected EPR (ED-EPR) and DEER measurements were carried out as a function of time after the delivery into the cells.

Figure 2 presents the 10 K W-band ED-EPR spectrum of ubiquitin D39C/E64C labeled with DO3MA-3BrPy-Gd<sup>III</sup> recorded in vitro (frozen solution) and in HeLa cells. The width of the central transition (full width at half height),

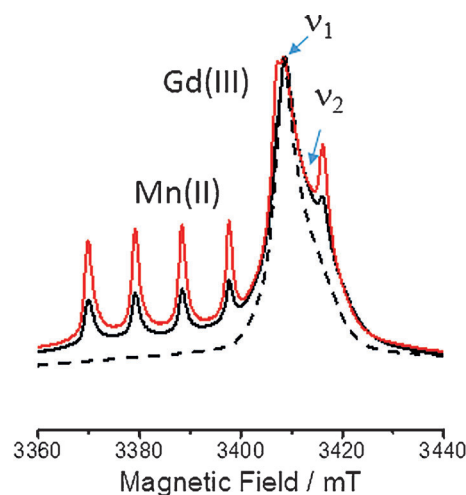


**Figure 2.** The central transition region of the 10 K W-band ED-EPR spectrum of ubiquitin D39C/E64C-DO3MA-3BrPy-Gd<sup>III</sup> in vitro (dashed line) and in cells, frozen 2 hours after delivery by hypotonic swelling (red) and 5 hours after delivery by electroporation (black), respectively. The positions of the pump ( $\nu_1$ ) and observe ( $\nu_2$ ) frequencies are denoted by arrows.

180 MHz, is larger than that of the maleimide-DOTA-Gd<sup>III</sup> label (50 MHz).<sup>[10b]</sup> This difference is attributed to the larger zero-field splitting (ZFS) arising from the lower symmetry around the Gd<sup>III</sup> induced by the coordination of the pyridyl nitrogen. Notably, strong cellular Mn<sup>II</sup> EPR signals are present in the in-cell samples.

DEER measurements on ubiquitin D39C/E64C-DO3MA-3BrPy-Gd<sup>III</sup>, both in frozen solution and in frozen HeLa cells, are presented in Figure 3. The position of the observe and pump pulses are indicated in Figure 2 and the experimental details are given in the Supporting Information.

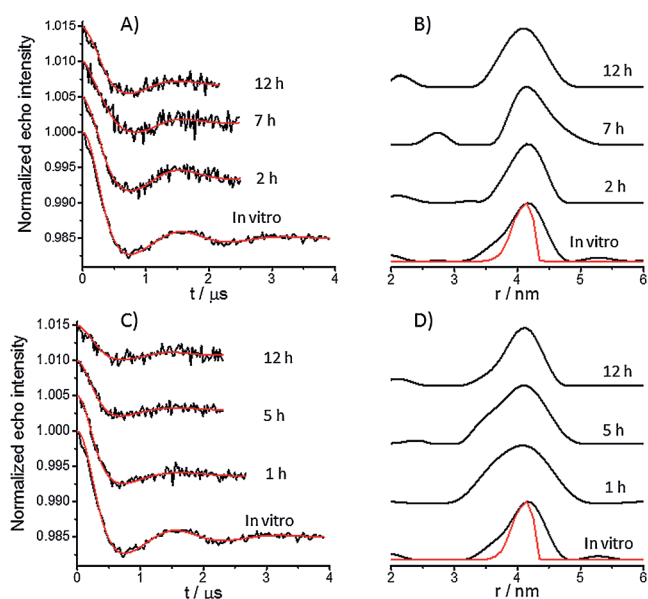


**Figure 3.** W-band DEER data after background correction of D39C/E64C-DO3MA-3BrPy-Gd<sup>III</sup> in vitro (bottom trace in each panel) and inside HeLa cells at different times after delivery by hypotonic swelling A) and electroporation C) along with the fits obtained using DeerAnalysis.<sup>[24]</sup> B) and D) are the distance distributions derived from the DEER traces in (A) and (C), respectively. All traces were shifted for clarity. The primary data are given in the Figure S7. The red traces in (B) and (D) correspond to the calculated distance distribution using MtsslWizzard,<sup>[27]</sup> and are depicted in both panels for better comparison with the in-cell measurements.

The four-pulse DEER trace of ubiquitin D39C/E64C-DO3MA-3BrPy-Gd<sup>III</sup> in vitro (75  $\mu$ M) is shown in Figure 3 A (bottom trace); clear modulations with a modulation depth,  $\lambda$ , of 1.5% are observed. This  $\lambda$  value is lower than that observed for ubiquitin labeled with maleimide-DOTA-Gd<sup>III</sup> (5%)<sup>[10b]</sup> owing primarily to the broader central transition of DO3MA-3BrPy-Gd<sup>III</sup>. The distance distribution derived from the DEER trace using DeerAnalysis,<sup>[24]</sup> shown in Figure 3 B at the bottom, has a maximum at 4.2 nm and a width at half height of 0.7 nm (a standard deviation of 0.37 nm). For this distance and the EPR central transition linewidth of 180 MHz we do not expect significant broadening owing to the failure of the weak coupling approximation used in the data analysis.<sup>[25]</sup> This compares favorably to a width of 0.5 nm (0.34 standard deviation) obtained for a rigid ruler molecule bearing two Gd<sup>III</sup>-PyMTA complexes and a Gd<sup>(III)</sup>-Gd<sup>(III)</sup>

distance of 4.3 nm<sup>[25]</sup> (see Figure S8). Considering that the labeling sites in the protein are not on a rigid secondary element, this difference is expected and is likely to originate from the protein flexibility. The reported distance distribution widths measured for the ubiquitin S20C/G35C mutant with MTSSL<sup>[5a]</sup> and maleimide-DOTA,<sup>[10b]</sup> were both 1.5 nm. This is significantly larger than for the D39C/E64C conjugated DO3MA-3BrPy-Gd<sup>III</sup> sample, with the reservation that the labeling sites are different.

To account for the distance distributions, we used the ubiquitin crystal structure<sup>[26]</sup> and anchored the DO3MA-3BrPy-Gd<sup>III</sup> complex to the sidechains of cysteines incorporated at positions 39 and 64 (see the Supporting Information and Figure S9 for details). The Gd<sup>III</sup>-Gd<sup>III</sup> distance was obtained using MtsslWizzard<sup>[27]</sup> for random variations of the torsion angles of the cysteine sidechains at the ligation sites with the paramagnetic tag, whereas all other structural segments were treated as a rigid body. The obtained distance distribution, shown in Figures 3 B and D as red traces, has a maximum at 4.1 nm, which is in excellent agreement with the experimental results.

The in-cell DEER data of D39C/E64C DO3MA-3BrPy-Gd<sup>III</sup> delivered into HeLa cells are shown in Figure 3 as well. To test the stability of DO3MA-3BrPy-Gd<sup>III</sup>-conjugated ubiquitin in living HeLa cells after hypotonic swelling and electroporation delivery, the cells were incubated for different times in the cell media (see the Supporting Information) and then frozen for ED-EPR and DEER measurements. For hypotonic swelling two-hour incubation was found to be sufficient for full cell recovery,<sup>[10b,23]</sup> whereas for electroporation delivery five hours are needed.<sup>[10a]</sup> The similar in vitro and in-cell Gd<sup>III</sup>-Gd<sup>III</sup> distance distributions indicate that the structure of ubiquitin reported by the D39C/E64C spin pair is essentially unchanged in cells. There are some differences in the distance distribution width for the proteins delivered by the different methods, of which electroporation produces a wider distribution for most samples. The data quality however is not sufficient for drawing unambiguous conclusions from this observation. In terms of the DEER modulation depth we observe a general reduction for the in-cell protein samples compared to the in vitro ones. Moreover, for hypotonic swelling, the modulation depth changed from 1.1% after 2 h to 0.9% after 7 h and to 0.8% after 12 h. For the electroporation delivery, the 1 h sample resulted in a modulation depth of 1.2%, which decreased to 0.7% for 5 h and to 0.5% after 12 h. The presence of cellular Mn<sup>II</sup> contributes to the background decay and reduces the modulation depth, but it does not affect the modulation frequency, that is, the distance distribution. This will be discussed further later.

The ED-EPR spectra of in-cell samples (Figure S10) reveal a decrease of the intensity of the Gd<sup>III</sup> signal with incubation time relative to the Mn<sup>II</sup> signal. We used these EPR spectra to estimate the in-cell Gd<sup>III</sup> concentration. The in-cell ED-EPR spectra were simulated as a superposition of two spectra: one corresponding to the in-cell Mn<sup>II</sup> background, which was obtained from the spectrum of cells without the delivered protein, and the other corresponding to the delivered protein, obtained from the in vitro sample with

the known concentration. The bulk Gd(III) concentration, namely, the concentration in the total volume of the sample, was then estimated from the relative weight of the above two spectra. (see Figure S10). We then estimated the in-cell Gd<sup>III</sup> concentration, which is higher than the bulk concentration because the cells do not comprise 100% of the sample volume, taking into account the number of cells in the sample and the cell volume (see the Supporting Information for details). The dependence of the Gd<sup>III</sup> bulk and in-cell concentrations on the incubation time for the two delivery methods is shown in Figure 4. A continuous decrease from 2 to 12 h is observed for hypotonic swelling and the in-cell concentration after 12 h was estimated to be about 5  $\mu\text{M}$  (corresponding to two Gd<sup>III</sup> per ubiquitin, which is equal to  $[\text{Gd}^{\text{III}}] = 10 \mu\text{M}$ ). For electroporation, more protein was delivered into the cell and the decrease in Gd<sup>III</sup> concentration in the cell with time was milder, and obvious changes were observed after 5 h after the delivery.

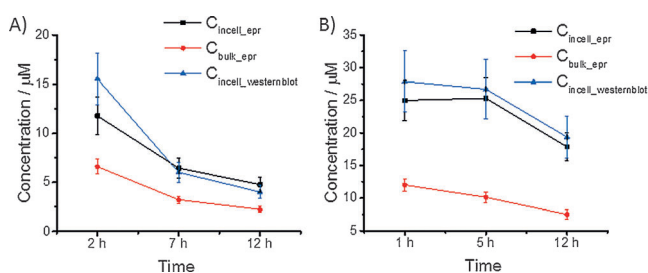


**Figure 4.** In-cell (black) and bulk (red) concentrations of ubiquitin D39C/E64C-DO3MA-3BrPy-Gd<sup>III</sup> determined by EPR spectroscopy and Western blots (blue) as a function of incubation time after delivery. A) Hypotonic swelling delivery. B) Electroporation delivery. Note that the Gd<sup>III</sup> concentration determined by EPR corresponds to 0.5  $[\text{Gd}^{\text{III}}]$ , which matches the protein concentration.

We also determined the in-cell ubiquitin concentration using Western blots (see Figure S11), and the results presented in Figure 4 show that there is a reduction in the concentration of monomeric ubiquitin in the cell with incubation time. The agreement between the in-cell concentrations determined from the EPR spectra and the Western blots is rather good, considering the error bars.

Using the spectral deconvolution shown in Figure S10, we estimated the relative contributions of the Gd<sup>III</sup> and Mn<sup>II</sup> signals at the observer frequency and found that they correlate closely with the change in the modulation depth for both delivery methods (see Figure S12). This indicates that there is no significant leakage of Gd<sup>III</sup> from the tag nor is there a significant detachment of the tag from the protein. The reduction in the modulation depth is mostly due to the reduction in the in-cell protein concentration and the presence of overlapping signals of Mn<sup>II</sup>. The former might be due to extrusion of the delivered spin-labeled proteins from the cells during incubation and maybe other degradation processes.

In summary, we presented a new Gd<sup>III</sup> spin label (DO3MA-3BrPy-Gd<sup>III</sup>) with a rigid tether, a high Gd<sup>III</sup> binding constant and high reactivity towards protein thiols

that can be efficiently attached to a protein. The new Gd<sup>III</sup> spin label demonstrated its excellent performance in W-band in-cell DEER measurements down to 5–10  $\mu\text{M}$  of in-cell protein concentrations with accumulation times within 20 h. Ubiquitin does not produce well resolved <sup>15</sup>N-HSQC NMR spectra in cells because the non-specific interactions with cellular constituents broaden NMR signals.<sup>[28]</sup> Our in vitro and in-cell DEER results indicate that these non-specific interactions do not affect the protein conformation as reported herein by the spin labeled D39C/E64C mutant. The high stability of this new and rigid Gd<sup>III</sup> spin label up to 12 h in living HeLa cells, along with its relatively small size and the high efficiency of its conjugation to protein cysteine residues is likely to find wide applications in delineating the structure and interactions of proteins in cells using DEER and NMR methods.

### Acknowledgements

This work was supported by Major National Scientific Research Projects (2013CB910201 and 2016YFA0501202), the National Natural Science Foundation of China (21473095 and 21273121) to X.-C.S and the Israel Science Foundation (ISF grant number. 334/14) to D.G. This research was made possible in part by the historic generosity of the Harold Perlman Family (D.G.). D. G. holds the Erich Klieger Professorial Chair in Chemical Physics. We thank Aleksei Litvinov for carrying out the modeling with MtsslWizzard. D.G. thanks Phil Selenko for his help with the electroporation protocol and for many helpful discussions. The help of Yoav Barak regarding the biochemical aspects of the work is highly appreciated and so are discussions with Ami Navon regarding the biochemical aspects of the work.

### Conflict of interest

The authors declare no conflict of interest.

**Keywords:** EPR spectroscopy · protein dynamics · protein structures · spin labels · structure elucidation

- [1] a) D. I. Freedberg, P. Selenko, *Annu. Rev. Biophys.* **2014**, *43*, 171–192; b) F.-X. Theillet, A. Binolfi, T. Frembsen-Kesner, K. Hingorani, M. Sarkar, C. Kyne, C. Li, P. B. Crowley, L. Gierasch, G. J. Pielak, A. H. Elcock, A. Gershenson, P. Selenko, *Chem. Rev.* **2014**, *114*, 6661–6714.
- [2] E. Luchinat, L. Banci, *J. Biol. Chem.* **2016**, *291*, 3776–3784.
- [3] a) G. Jeschke, Y. Polyhach, *Phys. Chem. Chem. Phys.* **2007**, *9*, 1895–1910; b) G. Jeschke, *Annu. Rev. Phys. Chem.* **2012**, *63*, 419–446.
- [4] T. Schmidt, M. A. Wälti, J. L. Baber, E. J. Hustedt, G. M. Clore, *Angew. Chem. Int. Ed.* **2016**, *55*, 15905–15909; *Angew. Chem.* **2016**, *128*, 16137–16141.
- [5] a) R. Igarashi, T. Sakai, H. Hara, T. Tenno, T. Tanaka, H. Tochio, M. Shirakawa, *J. Am. Chem. Soc.* **2010**, *132*, 8228–8229; b) M. Azarkh, O. Okle, P. Eyring, D. R. Dietrich, M. Drescher, J.

- Magn. Reson.* **2011**, *212*, 450–454; c) I. Krstić, R. Haensel, O. Romainczyk, J. W. Engels, V. Dötsch, T. F. Prisner, *Angew. Chem. Int. Ed.* **2011**, *50*, 5070–5074; *Angew. Chem.* **2011**, *123*, 5176–5180.
- [6] a) B. Joseph, A. Sikora, E. Bordignon, G. Jeschke, D. S. Cafiso, T. F. Prisner, *Angew. Chem. Int. Ed.* **2015**, *54*, 6196–6199; *Angew. Chem.* **2015**, *127*, 6294–6297; b) B. Joseph, A. Sikora, D. S. Cafiso, *J. Am. Chem. Soc.* **2016**, *138*, 1844–1847.
- [7] a) M. J. Schmidt, A. Fedoseev, D. Summerer, M. Drescher, *Methods Enzymol.* **2015**, *563*, 483–502; b) A. P. Jagtap, I. Krstić, N. C. Kunjir, R. Hansel, T. F. Prisner, S. T. Sigurdsson, *Free Radical Res.* **2015**, *49*, 78–85; c) M. J. Schmidt, J. Borbas, M. Drescher, D. Summerer, *J. Am. Chem. Soc.* **2014**, *136*, 1238–1241.
- [8] J. J. Jassoy, A. Berndhauser, F. Duthie, S. P. Kuhn, G. Hage-lueken, O. Schiemann, *Angew. Chem. Int. Ed.* **2017**, *56*, 177–181; *Angew. Chem.* **2017**, *129*, 183–187.
- [9] A. Feintuch, G. Otting, D. Goldfarb, *Methods Enzymol.* **2015**, *563*, 415–457.
- [10] a) F. X. Theillet, A. Binolfi, B. Bekei, A. Martorana, H. M. Rose, M. Stuver, S. Verzini, D. Lorenz, M. van Rossum, D. Goldfarb, P. Selenko, *Nature* **2016**, *530*, 45–50; b) A. Martorana, G. Bellapadrona, A. Feintuch, E. Di Gregorio, S. Aime, D. Goldfarb, *J. Am. Chem. Soc.* **2014**, *136*, 13458–13465.
- [11] B. Q. Shen, K. Xu, L. Liu, H. Raab, S. Bhakta, M. Kenrick, K. L. Parsons-Reponte, J. Tien, S. F. Yu, E. Mai, D. Li, J. Tibbitts, J. Baudys, O. M. Saad, S. J. Scales, P. J. McDonald, P. E. Hass, C. Eigenbrot, T. Nguyen, W. A. Solis, R. N. Fuji, K. M. Flagella, D. Patel, S. D. Spencer, L. A. Khawli, A. Ebens, W. L. Wong, R. Vandlen, S. Kaur, M. X. Sliwkowski, R. H. Scheller, P. Polakis, J. R. Junutula, *Nat. Biotechnol.* **2012**, *30*, 184–189.
- [12] M. Qi, A. Gross, G. Jeschke, A. Godt, M. Drescher, *J. Am. Chem. Soc.* **2014**, *136*, 15366–15378.
- [13] a) Y. Yang, Q. F. Li, C. Cao, F. Huang, X. C. Su, *Chem. Eur. J.* **2013**, *19*, 1097–1103; b) F. H. Ma, J. L. Chen, Q. F. Li, H. H. Zuo, F. Huang, X. C. Su, *Chem. Asian J.* **2014**, *9*, 1808–1816.
- [14] F. C. Mascali, H. Y. V. Ching, R. M. Rasia, S. Un, L. C. Tabares, *Angew. Chem. Int. Ed.* **2016**, *55*, 11041–11043; *Angew. Chem.* **2016**, *128*, 11207–11209.
- [15] G. T. Hermanson, *Bioconjugate techniques*, Elsevier, Academic Press, Amsterdam, **2008**.
- [16] Y. Yang, J.-T. Wang, Y.-Y. Pei, X.-C. Su, *Chem. Commun.* **2015**, *51*, 2824–2827.
- [17] K. L. Gempf, S. J. Butler, A. M. Funk, D. Parker, *Chem. Commun.* **2013**, *49*, 9104–9106.
- [18] a) N. Toda, S. Asano, C. F. Barbas, *Angew. Chem. Int. Ed.* **2013**, *52*, 12592–12596; *Angew. Chem.* **2013**, *125*, 12824–12828; b) D. Zhang, N. O. Devarie-Baez, Q. Li, J. R. Lancaster, M. Xian, *Org. Lett.* **2012**, *14*, 3396–3399.
- [19] A. Dondoni, A. Marra, *Chem. Soc. Rev.* **2012**, *41*, 573–586.
- [20] a) F. Yang, X. Wang, B.-B. Pan, X.-C. Su, *Chem. Commun.* **2016**, *52*, 11535–11538; b) T. Müntener, D. Häussinger, P. Selenko, F.-X. Theillet, *J. Phys. Chem. Lett.* **2016**, *7*, 2821–2825.
- [21] J. L. Chen, X. Wang, F. Yang, C. Cao, G. Otting, X.-C. Su, *Angew. Chem. Int. Ed.* **2016**, *55*, 13744–13748; *Angew. Chem.* **2016**, *128*, 13948–13952.
- [22] C. Schmitz, M. J. Stanton-Cook, X.-C. Su, G. Otting, T. Huber, *J. Biomol. NMR* **2008**, *41*, 179.
- [23] E. Di Gregorio, G. Ferrauto, E. Gianolio, S. Aime, *Contrast Media Mol. Imaging* **2013**, *8*, 475–486.
- [24] G. Jeschke, V. Chechik, P. Ionita, A. Godt, H. Zimmermann, J. Banham, C. R. Timmel, D. Hilger, H. Jung, *Appl. Magn. Reson.* **2006**, *30*, 473–498.
- [25] A. Dalaloyan, M. Qi, S. Ruthstein, S. Vega, A. Godt, A. Feintuch, D. Goldfarb, *Phys. Chem. Chem. Phys.* **2015**, *17*, 18464–18476.
- [26] R. Ramage, J. Green, T. W. Muir, O. M. Ogunjobi, S. Love, K. Shaw, *Biochem. J.* **1994**, *299*, 151.
- [27] G. Hage-lueken, R. Ward, J. H. Naismith, O. Schiemann, *Appl. Magn. Reson.* **2012**, *42*, 377–391.
- [28] T. Sakai, H. Tochio, T. Tenno, Y. Ito, T. Kokubo, H. Hiroaki, M. Shirakawa, *J. Biomol. NMR* **2006**, *36*, 179–188.

Manuscript received: November 11, 2016

Revised: January 2, 2016

Final Article published: ■ ■ ■ ■ ■ ■ ■ ■ ■ ■

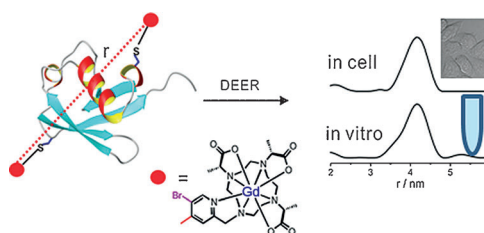
## Communications



## Structure Elucidation

Y. Yang, F. Yang, Y. J. Gong, J. L. Chen,  
D. Goldfarb,\* X.-C. Su\* — ■■■■—■■■■

A Reactive, Rigid Gd<sup>III</sup> Labeling Tag for In-Cell EPR Distance Measurements in Proteins



**Distance measurements:** A reactive and rigid Gd<sup>III</sup> spin label showed excellent performances in distance measurements using the double electron–electron resonance (DEER) method in vitro and in

cells. High-quality DEER data could be obtained in HeLa cells at protein concentrations as low as 5–10  $\mu\text{M}$  up to 12 h after the delivery of proteins.